A study of the trace gas columns of O_3, NO_2 and HCHO over Africa in September 1997†

Julian Meyer-Arnek,*‡ **Annette Ladstätter-Weißenmayer,*** **Andreas Richter,**
Folkard Wittrock and John P. Burrows*

Institut für Umweltphysik, Universität Bremen, Otto-Hahn-Allee 2, 28359 Bremen.
E-mail: julian@iup.physik.uni-bremen.de; lad@iup.physik.uni-bremen.de;
burrows@iup.physik.uni-bremen.de

Retrievals of trace gas columns from the measurements of backscattered radiation by GOME (Global Ozone Monitoring Experiment) show that enhanced tropospheric columns of ozone (O_3), nitrogen dioxide (NO_2) and formaldehyde (HCHO), over the African continent occur frequently. This study focuses on the behaviour of trace gases over Africa in September 1997, a period impacted by the strongest known El Niño phase of the ENSO. It investigates our qualitative and quantitative understanding of the retrieved tropospheric trace gas column densities. The emissions of NO_x and volatile organic compounds (VOC) from biomass burning, biogenic sources and lightning and their photochemical transformation have been investigated. By performing a trajectory analysis, the transport of air masses from the different emission regions was analysed and the potential atmospheric spatial distribution determined. BRemen's Atmospheric PHOtochemical model (BRAPHO) was applied to compute the chemistry along a large number of trajectories. From these results, tropospheric column amounts of O_3, NO_2 and HCHO were derived. Tropospheric trace gas columns retrieved from GOME measurements and those calculated are in reasonable agreement. Their general spatial extent was similar in the lower troposphere but the modeled trace gas columns in the upper troposphere were located south of the retrieved columns. We attribute this behaviour to uncertainties in the ERA-40 meteorological data in the upper troposphere. The significance of biomass burning and of biogenic emissions with respect to HCHO columns over Africa was investigated. The analysis reveals that the total amounts of HCHO generated over Africa during September 1997 as a result of biomass burning and biogenic emissions are similar. However the HCHO from biogenic sources has the highest specific columns and these are located close to their source. In comparison the HCHO from biomass burning is predicted to be produced and transported over a much wider area. Overall all the emission processes mix together to produce the plume of O_3.

1. Introduction

The Global Ozone Monitoring Experiment, GOME, measures the back scattered solar radiation leaving the top of the atmosphere.[1] Inversion of GOME data yields information on trace gas columns. Retrievals from GOME measurements frequently reveal strong enhancements of tropospheric trace gas columns of ozone (O_3), nitrogen dioxide (NO_2) and formaldehyde (HCHO), over Africa, the tropical Atlantic and parts of the Indian Ocean. The plumes of O_3 in the tropics and in particular over Africa, identified by the TOMS (Total Ozone Mapping Spectrometer) instrument and from O_3 sondes have been the source of much recent discussion (refs. 2 and 3, and references therein). Over the African continent, several different processes have a significant impact on the regional and global air quality: biomass and biofuel burning, biogenic emissions and pollution from the combustion of fossil fuel (for example from road traffic).[4] Industrial processes are considered in Africa only to be of minor significance.[5] One exception is however the industrialised parts of South Africa, which emit significant amounts of NO_x ($= NO + NO_2$) and sulfur dioxide, SO_2. These emissions have not been considered explicitly in this study. The impact of these emissions needs a separate investigation.

Biomass burning, initiated in order to clear land for agricultural purposes, is a well-known significant source of O_3 precursors such as NO_x and volatile organic compounds, VOC. The emissions from biomass burning are now accepted to affect the atmosphere at local, regional and global scales.[6–8] In addition to particulate matter, the major gases produced by biomass burning include carbon dioxide (CO_2), carbon monoxide (CO), methane (CH_4), HCHO, NO_x and ammonia (NH_3). The summer smog was first identified in Los Angeles in the late 1940s. The emissions from anthropogenic activity are oxidised in a photo-initiated chain reaction producing O_3 and many other intermediates. As is now well known, the combination of sunlight and mixtures of CH_4, CO, nonmethane hydrocarbons (NMHC) and NO_x in the atmosphere results in the photochemical production of tropospheric O_3 at global scales.[9] As CO_2, CH_4, and O_3 absorb strongly in the infrared spectral region but only weakly in the visible, the emissions from biomass burning also contribute to global climate change. The abundance of tropospheric O_3, which is itself an oxidant, determines to a significant extent the amount of the most important tropospheric oxidising agent, the hydroxyl radical, OH, and also the peroxy radicals (hydroxyperoxy radical, HO_2, and the organic peroxy radicals, RO_2).[10] The lifetimes of ozone precursors and of ozone itself are sufficiently long that they can be transported hundreds or even thousands of kilometres away from the emission source region before being chemically destroyed or deposited.[11]

Over Africa significant amounts of NMHC are emitted by vegetation. The global emission of different VOC from vegetation is estimated to amount to approximately 1150 Tg y^{-1} [12] and is around ten times the amount of the anthropogenic VOC emissions. Isoprene (C_5H_8) alone accounts for about 500 Tg y^{-1} and is the largest single VOC emission into the boundary layer by the biosphere in the tropics (*e.g.* ref. 12).

HCHO is produced in the oxidation of methane, CH_4, and NMHC. In the clean remote atmosphere the amount of HCHO from the oxidation of CH_4 is relatively small being of the order of 200 pptv. However as a result of the photochemical initiated oxidation of hydrocarbon of either biogenic or anthropogenic origin, relatively large mixing ratios of HCHO in the range 0.3–10 ppbv are often encountered. In addition HCHO is emitted directly from biomass burning, as a result of the partial oxidation of organic compounds and also produced in the plume from biomass burning as a result of the oxidation of VOC/NMHC.

The photochemically initiated oxidation of hydrocarbons requires a sufficient amount of NO_x to be effective. The chain length of the oxidation depends critically on the amount of NO_x. At low NO_x the chain length is reduced by competition between the reactions of the peroxy radicals with NO and their self-reactions. At high NO_x termination reactions such as the reaction of OH with NO_2 also reduce the chain length. Thus the rate of formation of HCHO is a non-linear function of the chemical conditions. However overall elevated amounts of HCHO are an indicator of the oxidation of biogenic VOC and biomass burning.
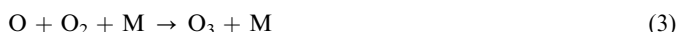
Biogenic emissions of highly reactive VOC are a particularly important source of HCHO in the planetary boundary layer and the lower troposphere. Isoprene is the largest biogenic emission, and as a hemiterpene contains five carbon atoms and has the potential to generate up to five molecules of HCHO. However isoprene has several competing oxidation pathways and as a result typically

1.5 to 2.25 molecules of HCHO are expected to be formed by the oxidation of one isoprene molecule depending on the NO_x loading of the atmosphere.[11] The reaction of isoprene with OH is fast, leading to an isoprene lifetime in the order of about half an hour under tropical conditions. As a result the isoprene oxidation occurs close to its sources. Similarly the shorter-lived oxidation products from isoprene are localised close to the isoprene source region.

In contrast to the reactive biogenic VOC emissions, many of the hydrocarbons emitted by biomass burning have significantly longer lifetimes (*e.g.* $\tau_{C_2H_6} = 10$ days, $\tau_{C_2H_4} = 6$ h and $\tau_{CH_4} = 1$ y). As a result of the long chemical lifetime of such species, they are transported and oxidised over long distances in the troposphere.

There are several sources of NO_x in the troposphere: combustion processes, lightning and surface emissions from the degradation of NO_3^- and NH_4^+ in soils. With the exception of aircraft emissions, the combustion of fossil fuel and biomass/biofuel burning takes place close to the Earth's surface in the planetary boundary layer. In the upper troposphere lightning is considered to be a significant source of NO_x. Estimates of the amount of NO_x released by lightning vary between 2 to 20 Tg y^{-1}.[12] In this study the soil emissions have not been considered in detail. This is because for the conditions of September 1997, this emission is regarded to be relatively small.

The retrievals of GOME yield the tropospheric distribution of NO_2 rather than NO_x. As a result of the fast photochemical cycle involving the reaction NO with O_3, during daytime a photochemical stationary state of NO and NO_2 is often achieved:

$$NO + O_3 \rightarrow NO_2 + O_2 \tag{1}$$

$$NO_2 + h\nu \, (\lambda < 404 \text{ nm}) \rightarrow NO + O \tag{2}$$

$$O + O_2 + M \rightarrow O_3 + M \tag{3}$$

This do nothing cycle would not result in the production of O_3. However the reaction of NO with peroxy radicals, as noted above, is of critical significance for the O_3 production since it changes the ratio of NO_2 to NO and as a result O_3 is generated. The reactions of halogen oxides with NO also change the ratio of NO_2 to NO, but the halogen atoms generated react with O_3 to regenerate the halogen oxide. To use the retrieved tropospheric columns of NO_2 as a measure of NO_x emissions, the ratio of $[NO_2]/[NO_x]$ needs to be estimated.

This study focuses on an episode of enhanced trace gas columns over Africa, which was observed in September 1997. The behaviour of the trace gases in 1997 was not untypical. However the strong ENSO (El Niño–Southern Oscillation) and related low rainfall in the Horn of Africa probably resulted in additional biomass burning. For the study the location of the processes leading to the emission of NO_x and precursors of HCHO and O_3 were identified. The transport of trace gases from the source regions was analysed by the trajectory model Traj.x. To account for chemical transformation during transport, BRemen's Atmospheric PHOtochemical model (BRAPHO) simulated the chemistry taking place along a large number of trajectories and the distribution of the total column of trace gases was determined. These were then compared with those retrieved from GOME. Finally the relative importance of biomass burning and biogenic emissions for the observed columns of O_3, NO_2 and HCHO was examined.

2. The retrieval of trace gas columns from GOME

The GOME instrument was launched in April 1995 onboard the European Research Satellite 2 (ERS-2) into a sun-synchronous orbit at a mean altitude of 795 km. The satellite, whose orbit is in a descending mode, crosses the equator at 10:30 am local time. GOME is a nadir-scanning double-monochromator measuring the sun light scattered from the Earth's atmosphere and surface in the wavelength region of 240 to 790 nm at a moderate spectral resolution of 0.17 to 0.33 nm. GOME also measures the extraterrestrial solar irradiance. The difference between the earthshine radiance and the extraterrestrial irradiance yield information about absorption, emission and scattering processes, which occur in the Earth's atmosphere and at its surface. Details of the overall scientific objectives of GOME, instrument concept, and some scientific results are reported elsewhere.[1]

The atmospheric O_3, NO_2 and HCHO columns are derived from GOME measurements by applying the differential optical absorption spectroscopy (DOAS) technique. This well established technique relies on the separation of high frequency from low frequency spectral structures (ref. 1,

and references therein). Typically the natural logarithm of the ratio of the extra terrestrial solar irradiance and the radiance up welling from the top of the atmosphere is generated. The resultant atmospheric extinction spectra are determined by absorption and scattering in the earth's atmosphere and at the surface.

Spectral windows in the atmospheric extinction spectra are selected where gases or combinations of gases have clearly identifiable spectral structures. The spectral structures are fitted and the slant column density of the gases determined. To convert the slant column to a vertical column the air mass factor, AMF, is required. This describes the difference between the actual light path through the atmosphere and a geometric path in the vertical. AMF are calculated using radiative transfer models. The simplest DOAS approach is limited to spectral regions of relatively weak absorption, where AMF is constant over a given spectral window. More complicated approaches have to be used to take into account regions of strong absorption, which are then associated with a changing AMF.

The O_3 vertical column, used in this study is retrieved from a fitting window between 325 and 335 nm. The level-2 data product O_3 total column density were generated by the GOME Data Processor (GDP) system, provided by the German Remote Sensing Data Center (DFD). NO_2 and HCHO columns are retrieved from GOME-level-1b data at the Institute of Environmental Physics (IUP/IFE). NO_2 and HCHO slant columns are retrieved from the spectral windows between 425 and 455 nm between 337.5 and 359 nm, respectively.[13,14] A number of studies have been published focusing on the retrieval of HCHO from GOME data.[1,13–17]

As GOME is a nadir-viewing instrument, both tropospheric and stratospheric absorptions contribute to the total column amount identified in the slant column. The tropospheric trace gas columns (see Fig. 1(a) and 1(b)) are derived by applying the tropospheric excess method (TEM) or reference sector approach.[14,17–20] The TEM is based on the assumption that the columns of stratospheric trace gases such as NO_2 and O_3 are approximately constant at a given longitude. This is a large oversimplification but appears to work well for monthly composites in tropical and subtropical conditions for O_3 and to higher latitudes for NO_2. The total column densities retrieved on the same day at the same latitude over a tropospheric region, which is unpolluted, are used as an approximation for the sum of the stratospheric column and the background tropospheric column over a region of interest. The TEM analysis yielding the tropospheric excess column comprises three steps: (a) determination of the total slant column, (b) subtraction of the stratospheric contribution and the tropospheric background (slant column) and (c) division by the air mass factor to obtain the vertical column. The error on the resultant tropospheric excess O_3 is estimated to be ~ 4 DU.[21] The tropospheric excess columns of NO_2 can be retrieved with a fitting error of around 1×10^{15} molecule cm^{-2}.[14] The detection limit for a retrieval of HCHO total columns from GOME radiances is about 2.5×10^{15} molecule cm^{-2}. This corresponds to a HCHO layer, which extends from the ground to $z = 2$ km, having a mixing ratio of ~ 500 ppt.

The GOME ground scene is large, 320×40 km^2, and not optimal for tropospheric observations, because clouds frequently obscure the field of view. For this reason and to improve the effective signal to noise ratio, monthly composites of tropospheric excess columns for ground scenes selected for low cloud, typically $<10\%$ are often used for analysis purposes.

In order to determine the total tropospheric column from the excess column, the tropospheric column of trace gas at the location of the clean reference sector has to be estimated. In this work the clean Pacific has been used as the reference sector. The tropospheric O_3 has been estimated from a sonde climatology. The total column of NO_2 is small and the HCHO is determined from model estimates and measurements, which indicate a column having a mixing ratio of around 200 pptv.

3. Satellite remote sensing data

In this study the tropospheric columns of O_3, NO_2 and HCHO have been investigated for September 1997 over Africa. We have recently investigated the Indonesian emissions in the same period, when the ENSO was in an El Niño phase.[22] The ENSO resulted in low rainfall in Indonesia and the Horn of Africa, thereby increasing the potential for biomass burning. The Intertropical Convergence Zone, ITCZ, crosses the African continent at this time of year, separating the northern hemispheric from southern hemispheric air. On the Atlantic side of Africa it begins north of the equator but heads south before entering the Indian Ocean where it splits.
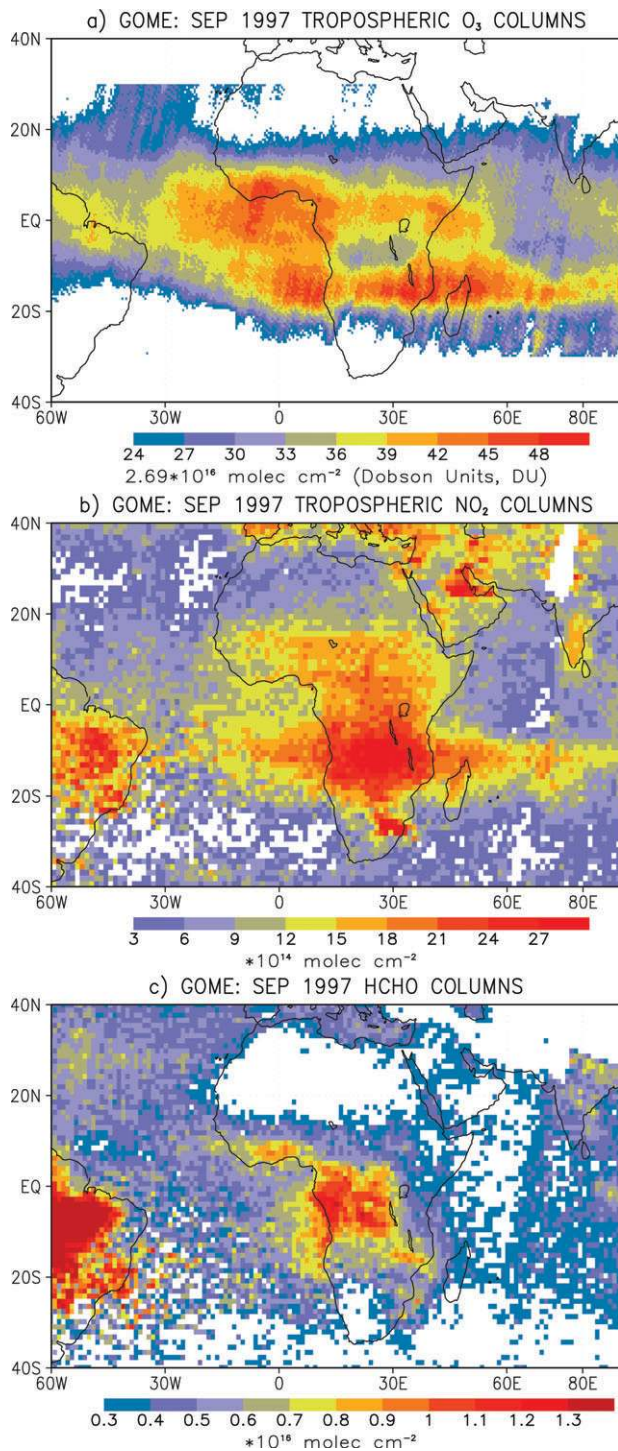
Fig. 1 The monthly composites of (a) total column of tropospheric O_3 (in DU), (b) the total column of NO_2 (in units of 10^{14} molecule cm^{-2}) (c) HCHO columns (in 10^{16} molecule cm^{-2}), for September 1997 as retrieved from GOME measurements.

Fig. 1 shows the monthly composites for the total tropospheric O_3, NO_2 and HCHO columns determined from GOME for September 1997. Enhanced columns of O_3, which are spread over the entire Central Africa, the equatorial Atlantic and part of the Indian Ocean, are shown in Fig. 1(a). The elevated columns of NO_2, which are largest in the regions of biomass burning in the southern parts of Central Africa, are shown in Fig. 1(b). The largest HCHO columns are located over the western parts of central Africa and the tropical Atlantic as shown; see Fig. 1(c).

Both biogenic emissions and biomass burning contribute to enhanced HCHO columns. HCHO columns, derived from GOME measurements, were large being up to 1.2×10^{16} molecule cm^{-2} over central Africa (see Fig. 1(c)), whereas HCHO columns over the barren Sahara desert are $< 2 \times 10^{15}$ molecule cm^{-2}.

In this study the regions of biomass burning are identified from the fire data derived from the ATSR-2 (Along Track Scanning Radiometer) instrument, which is, like GOME, aboard the ERS-2. ATSR measures the infrared radiation emitted from the top of the atmosphere. Hotspots detected during the night are assigned to be fires. These fire count data are provided by the European Space Agency (ESA).[23,24] By projecting all hotspots detected in September 1997 onto a global grid of $1.125° \times 1.125°$ the fire index shown in Fig. 2 is generated. Its unit is fire counts per $1.125° \times 1.125°$ per month. It reveals that biomass burning regions at this time of year are concentrated in the savannah regions of the eastern part of southern Africa as well as Amazon rain forest in South America. Fires, identified in the Persian Gulf area and the northern Sahara desert, are associated with oil production.[24]

In order to investigate and model the biogenic emissions of precursors of HCHO, knowledge of the vegetation type is required. In Fig. 3, the spatial distribution of the tropical rain forest and of woody savannah is plotted from a vegetation map, provided by the Flemish Institute of Research and Technology (VITO).[25] It is based on the classification of vegetation regimes (biome) defined by the International Geosphere–Biosphere Programme (IGBP). The tropical rain forest is denoted as 'evergreen broadleaf forest'. The original vegetation data set has a resolution of 1×1 km and was converted to a $1° \times 1°$ latitude $\times$ longitude grid. This was achieved by evaluating the area covered by each of the different biological regimes within one coarse ($1° \times 1°$) grid cell. The biological regime covering the largest fraction determines the regime of the coarse grid cell.

The biogenic emission of isoprene, the most abundant organic VOC, is known to be proportional to temperature, actinic flux and leaf area (e.g. see refs. 11 and 12). Consequently the dense tropical rain forests of Central Africa and South America, situated in regions of high temperatures and high actinic flux, account for a significant portion of the global isoprene emission. Moreover enhanced isoprene emission takes place in the transition region between the tropical rain forests and the savannah regions, which is referred to as woody savannah.
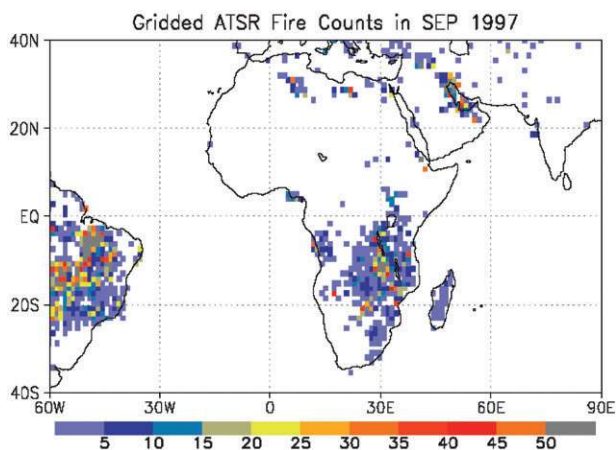

Fig. 2 Fire index derived from ATSR-algorithm 2 data for September 1997. It is given in fire counts per $1.125° \times 1.125°$ per month.
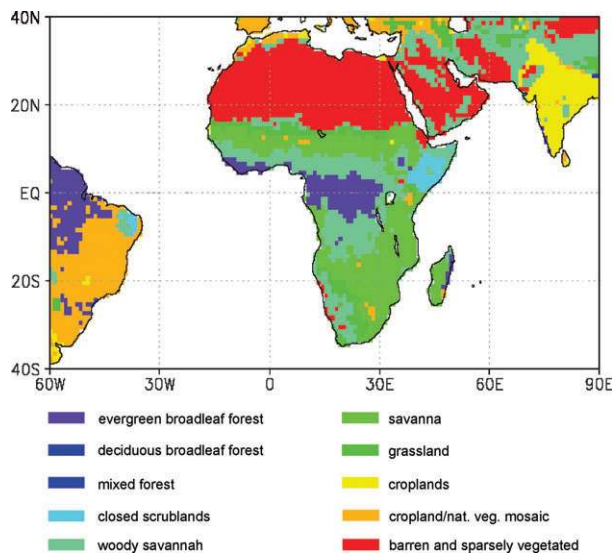
Fig. 3 Map of biological regimes (biomes) provided by the Flemish Institute for Research and Technology (VITO). The data set is converted from a 1 km by 1 km to a 1° by 1°-resolution.

In Fig. 4, the monthly mean HCHO column densities determined from GOME measurements are compared for the Congo Basin, defined as 5° N to 5° S and 10° E to 30° E, and for the region covering roughly Zambia, Zimbabwe and Mozambique, ZZM, defined as 10° S to 20° S and 25° E to 35° E. In September 1997 both regions have very significant columns of HCHO. The savannah region of the ZZM has a relatively large seasonal cycle with the highest values being in September, October and November and the lowest values in May, June and July 1997.

The seasonal behaviour shown in Fig. 4 reveals that the HCHO column over the Congo Basin remains elevated above 5×10^{15} molecule cm^{-2} throughout the whole year and follows the sun's annual cycle reaching maximum values during the equinoxes in March and September. This behaviour can qualitatively be understood by considering the annual cycle of isoprene emission. The savannah regions of east and central Africa have elevated HCHO columns in the burning season.
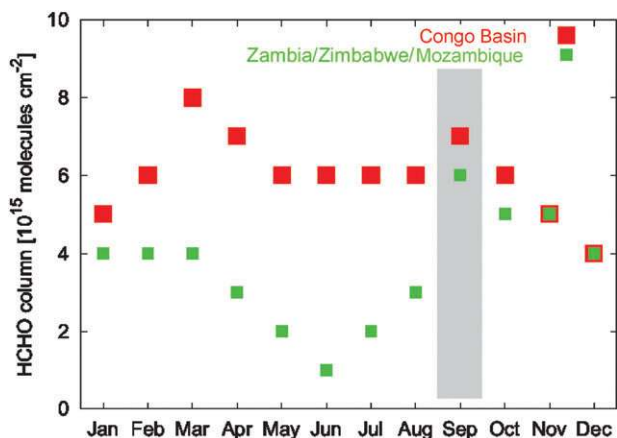

Fig. 4 Monthly mean HCHO columns over the Congo Basin (from 5° N to 5° S and from 10° E to 30° E) and over parts of Zambia, Zimbabwe and Mozambique (covering a region expanding from 10° S to 20° S and from 25° E to 35° E) as retrieved from GOME measurements for 1997. The September values are shaded in grey.

NO$_2$ has the shortest lifetime of the three trace gases retrieved from GOME. Biomass and biofuel burning, lightning and pollution produce it. The NO$_2$ emission from the mining region in South Africa is clearly visible in Fig. 1(b) as are the cities and oil producing regions of the Middle East. Similarly the large biomass burning over the Amazon rain forest is readily observed. As noted above these emissions are not the focus of this study but rather the large biomass burning emission and the impact of lightning over Africa. As a result of the pressure dependent reaction of OH with NO$_2$, the lifetime of NO$_2$ in the upper troposphere is longer than in the lower troposphere. In the troposphere NO$_2$ is transported westward in the lower atmosphere but also convected to the upper troposphere and transported eastwards. In spite of this longer lifetime the outflow of NO$_2$ from East Africa over Madagascar is probably indicating significant production of NO$_2$ from lightning.

Although the continuous NO$_x$ emission from soils and fossil fuel combustion are not insignificant, the distribution of the NO$_2$ column in September 1997 is dominated by biomass burning and lightning. For this study a lightning climatology based on 7 y of measurements performed by the Lightning Imaging Sensor (LIS) and the Optical Transient Detector (OTD) was applied. It reveals that the world's most intense lightning activity is located over the African Congo Basin.[25]

As a result of its relatively long lifetime of days to months,[11] and because it is produced in the plume from a continent, O$_3$ can be transported over large, even intercontinental, distances. The monthly composite for tropospheric O$_3$ columns shown in Fig. 1(a) for September 1997 is attributed to the photochemical oxidation of the emissions of VOC and NO$_x$ and their subsequent transport and chemical transformation. The outflow in the lower atmosphere biogenic emissions over the Congo Basin and from biomass burning results in O$_3$ being produced and transported westward. In comparison on the eastern side of Africa, O$_3$ is convected out of the boundary layer and subsequently transported eastwards across the Indian Ocean.

4. Analyses of air parcel trajectories

As part of our investigation of the distributions of trace gases in September 1997, the air parcel trajectories have been studied ignoring chemical transformation. The air parcel trajectories were calculated using Traj.x, which has been developed at the University of Bremen and is a kinematic trajectory model. It calculates the transport of air parcels using the meteorological wind fields by applying a fourth-order Runge–Kutta scheme. The meteorological data were taken from the European Centre for Medium-Range Weather Forecasts (ECMWF)'s 40 y reanalysis data set (ERA-40).

To investigate the transport from the source regions, trajectories have been calculated for each day of September 1997. The trajectories were initiated from regions, defined with a particular emission type, at 0000 UTC, 0600 UTC, 1200 UTC and 1800 UTC. For air parcels from biomass burning and biogenic regions, trajectories were started at pressure levels of 50, 100, 150 and 200 hPa below the pressure at ground level. For example assuming ground pressure of 900 hPa, trajectories are released at 850, 800, 750 and 700 hPa. All air parcels are then followed for 10 d. To account for lightning, which affects the upper troposphere, the trajectories representing lightning were released at pressure altitudes of 500, 400, 300 and 200 hPa, from locations where the strongest NO$_x$ emission from lightning is expected.[13]

For this study the trajectories are released on a $1° \times 1°$ latitude–longitude grid over the geographical location of the biomass burning, biogenic emission or lightning. Altogether about 230 000 trajectories were calculated for the conditions of September 1997. To interpret the general transport pattern occurring above Africa in September, a quantity called the trajectory density has been defined. This quantity is derived by projecting the current position of all trajectories released from the particular emission region into a three dimensional grid depending on longitude, latitude and altitude. Its horizontal resolution is $1.125° \times 1.125°$, and its vertical step is 50 hPa. The vertical extension spans from the ground to 50 hPa. For ease of comparing trajectory densities from different sources, the maximum value of this quantity is normalised to unity.

High values of the trajectory density indicate that many trajectories from the source region have travelled through a particular grid cell. Thus the trajectory density describes the patterns of transport.

Using the fire counts shown in Fig. 2 to define the region of the emissions from biomass burning, the resultant trajectories are distributed over a significant fraction of the east and south of the
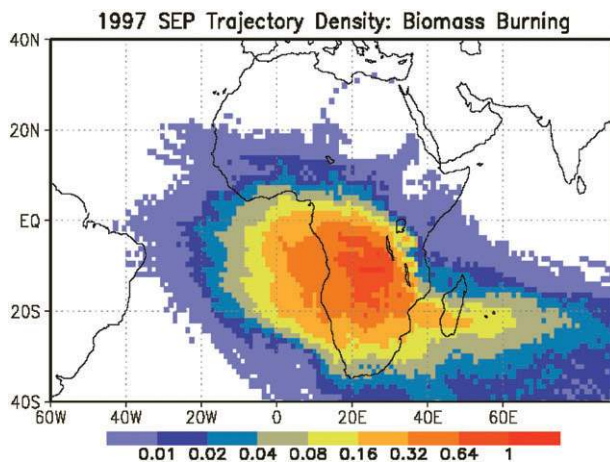
Fig. 5 Trajectory density of trajectories emerging from biomass burning located over Africa during September 1997.

African continent. Fig. 5 shows the vertically integrated trajectory density for air masses originating from the biomass burning areas. This distribution is explained by an analysis of the trajectories in three dimensions. At lower altitudes (*i.e.* below 700 hPa), the biomass burning emissions are advected westwards. A significant number of air parcels released from biomass burning are convected. These air parcels rise up to altitudes above about 500 hPa and are transported eastwards. Some of these are transported into the jet stream, which accounts for long range transport in the upper troposphere from Africa to Australia.

When comparing the trajectory density derived for the emissions from biomass burning with the retrieved tropospheric NO_2 columns (see Fig. 1(b)), the modeled eastward transport of the fire emissions appears to be shifted southward by about $10°$ latitude.

Fig. 6 shows the trajectory density for trajectories emerging from the tropical rain forest and woody savannah regions. Although some convection does takes place, it is clear that biogenic emissions, released from the dense tropical rain forests and from the savannah, remain predominantly at lower altitudes *i.e.* at pressures below about 700 hPa, being slowly advected in westerly directions towards the equatorial Atlantic. A small fraction of the air masses from the biogenic source region are convected and transported eastwards. As a result of this pattern of flow, biogenic
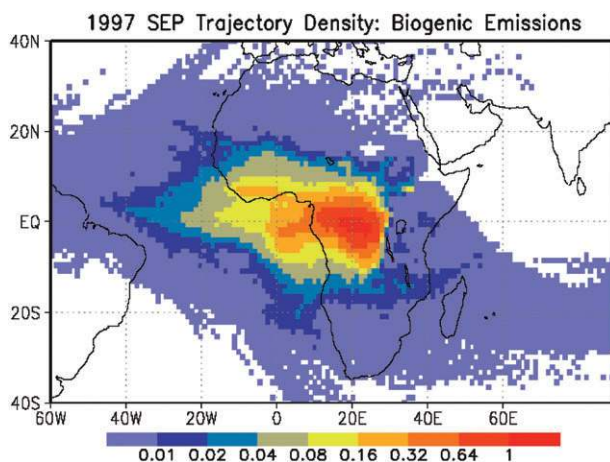

Fig. 6 Trajectory density for trajectories emerging from the tropical rain forest and woody savannah during September 1997.
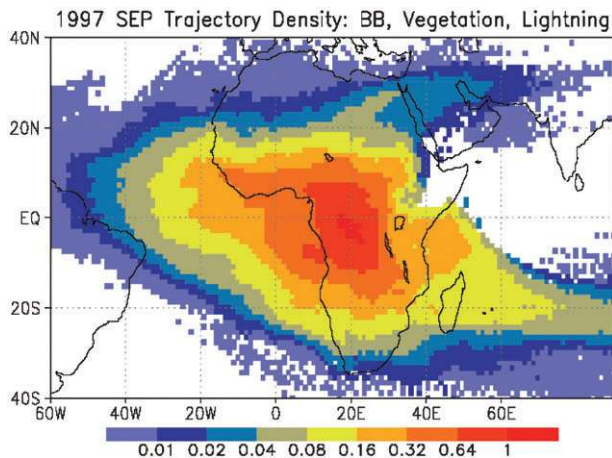
Fig. 7 Combined trajectory density of trajectories emerging from biomass burning, the dense tropical rain forest and lightning over the African Congo Basin.

emissions remain close to the vicinity of the tropical rain forest for a comparably long time *i.e.* in the order of days. This also implies that enhanced HCHO columns from the oxidation of biogenic emissions of NMHC/VOC are likely to be localised close to and downwind of the Congo Basin.

To assess the impact of the emissions from the localised biogenic emissions, the widespread biomass burning emissions and of lightning, the trajectory densities derived for all these processes were combined. This combined vertically integrated trajectory density is shown in Fig. 7.

The spatial distribution of the combined trajectory density is similar to the distribution of the overall spread of the plume of tropospheric O_3 column, retrieved from GOME measurements for September 1997. As noted for the comparison with NO_2, the maximum combined trajectory density is shifted towards the south compared with the O_3.

The difference in location between the observed plumes of NO_2 and O_3 and the location of the trajectory density in the Indian Ocean may be explained by a number of effects. One possibility is the regional variation of the strength of the NO_x emission from the biomass burning is not accurate, changing the position of the effective maxima of the plumes of O_3 and NO_2. Another possibility is that lightning may be distorting the distribution. However, the most likely cause of the differences are inaccuracies in the meteorological data set in the middle and upper troposphere. The strong outflow of trace gases from Africa, which occurs at the equinox, has been identified as resulting from the weakening of the meridional transport during the inter-monsoon period, which allows a strengthening of transport across the Indian Ocean.[25]

To approximate for the decay of HCHO concentration with increasing altitude, those trajectories emerging from areas of biomass burning and biogenic emission and residing below 500 hPa were combined. The results are shown in Fig. 8. The location of the maximum agrees qualitatively quite well with the spatial distribution of HCHO retrieved from GOME measurements during September 1997.

It is interesting to compare the observations of HCHO and NO_2, which are both produced by biomass burning. However the sources of NO_x are close to the fire, whereas HCHO is produced in the fire but also downwind of the fire as a result of the oxidation of hydrocarbons released from the fire. HCHO has a significantly longer chemical lifetime than NO_2. Nevertheless the spatial distribution of the HCHO plume is much less than the NO_2 plume. This implies a significant role for lightning production of NO_x.

5. Chemical modeling of the air above Africa in September 1997

In order to calculate tropospheric columns of trace gases for comparison with the retrieved trace gas columns from GOME, both the transport and the chemical transformations have to be taken into consideration. In this study BRAPHO has been used. The Lagrangian model, which is based on
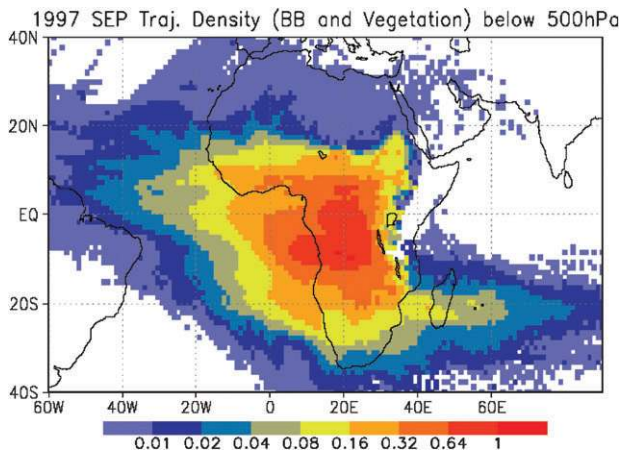
Fig. 8 Trajectory density of trajectories emerging from HCHO sources as biomass burning, dense tropical rain forest and woody savannah and residing below 500 hPa.

ASAD (A Self contained Atmospheric chemistry coDe),[28] computes the chemistry taking place in a closed air parcel, which does not undergo any exchange with its surroundings. The air mass is advected through the atmosphere along the calculated trajectories.

For computational efficiency, three-dimensional chemistry and transport models usually apply a parameterised and typically simple chemical scheme. The advantage of the Lagrangian box model approach, like that used in BRAPHO, is that the complex chemistry can be simulated. This implies that even branched oxidation chains, like the isoprene oxidation, do not need to be parameterised.

The chemistry occurring in the tropospheric boundary layer is nonlinear and complex. Large amounts of both NO_x (due to high temperatures in the flames) and VOC are released into the atmosphere from biomass burning, leading to strong ozone production. The tropical rain forest emits large amounts of VOC, mainly isoprene. Directly in the vicinity of the rain forest, the NO_x remains at relatively low levels (below 200 pptv). However up to 2ppb NO_2 have been measured over regions where biomass burning took place during the Transport and Atmosphere Chemistry near the Equator–Atlantic (TRACE-A) campaign, which was conducted in 1992.[29]

During the TRACE-A-campaign, airborne measurements at altitudes of about a few hundred metres to a few kilometres were conducted over Africa, South America and the Southern Atlantic Ocean. The subset of measurements performed at low altitudes (below 1000 m) over biomass burning represent the chemical composition of air masses being influenced by fires but being sufficiently far enough away from the complicated flame chemistry. TRACE-A composition measurements have been selected to represent the chemical situation in this study.

The chemistry used for this study is based on the detailed Master Chemical Mechanism (MCM) version 3.0 catalogue.[30] The oxidation pathways of all the species, which were measured during the TRACE-A-campaign (O_3, NO_2, CO, C_2H_2, ethyne, C_3H_8, propane, CH_3COCH_3, acetone, H_2O_2, hydrogen peroxide, HNO_3, nitric acid, PAN, peroxy-acetyl-nitrate) and C_5H_8, isoprene, and CH_4 are automatically extracted from this catalogue covering the complete tropospheric chemistry. The extraction algorithm ensures that all (intermediate) oxidation steps are included in the model's chemistry. The resulting chemistry scheme, which was used in this study, includes about 750 reactions of about 260 species. All species and all chemical reactions are listed in the electronic supplementary information (ESI).

Using this chemistry, the BRAPHO Lagrangian box model was computed along a large number of trajectories. All of these trajectories either start over regions where biomass burning takes place or over the dense tropical rain forests. The chemical model is initialised depending on the biological regime and the fire-index at the starting point of the trajectories. For this purpose, a two-dimensional initialisation matrix depending on the biome (see Fig. 3) and on the ATSR-fire index (see Fig. 2) is generated by matching the averaged fire count data and the biome data with the trace gas measurements performed during the TRACE-A-campaign.

The tropical rain forest is—on a global scale—the most important source of isoprene due to high temperatures and high actinic flux in the equatorial regions and its dense vegetation. Based on assumptions from Guenther *et al.*,[31] its averaged isoprene flux is estimated to account for up to 6 g C m^{-2} month^{-1}.[32] The average isoprene flux generated by woody savannah, the transitional regime between the tropical rain forest and the savannah, is estimated to yield for 2.7 to 5.4 g C m^{-2} month^{-1}.[32]

For the initialisation of a chemical box model (like BRAPHO), the knowledge of the volume mixing ratios is needed; trace gas fluxes cannot be directly used for the initialisation of the model. This is particularly important for the modeling of isoprene and its oxidation. To convert the isoprene flux into a volume mixing ratio, a steady state between its emission by plants and its dominant chemical loss due to the reaction with OH is assumed. A time-independent isoprene emission of 5.2 g C m^{-2} month^{-1} within the tropical rain forest leads to an isoprene mixing ratio of about 2 ppbv. When assuming an isoprene flux of 2.7 g C m^{-2} month^{-1}, which is reasonable for woody savannah, a volume mixing ratio of about 1 ppbv is obtained. Further, the strong diurnal dependence of the isoprene emission has to be taken into consideration. Only small amounts of isoprene are emitted during the night. Consequently all trajectories being released over the tropical rain forest during daytime are initialised with an isoprene loading of 4 ppb and those emerging woody savannah with an isoprene mixing ratio of 2 ppb. During the night the isoprene mixing ratio is reduced by two orders of magnitude in the model. The isoprene mixing ratios used are in reasonable agreement with measurements performed during EXPRESSO (EXPeriment for REgional Sources and Sinks of Oxidants) in 1996 in the tropical rain forest[33] and those performed by Sillman[34] in a forested area of the United States during summer. The latter observed isoprene volume mixing ratios of up to 6 ppbv during daytime and 0.02 ppbv during night time at the ground below the level of canopy.

Air masses being influenced by lightning are initialised by using upper-tropospheric TRACE-A-composites which have been identified as unpolluted. After the release of these air masses, which takes place at either 0000, 0600, 1200 or 1800 UTC, an emission of 500 pptv NO$_x$ into the box model was performed at 1500 local time. This accounts for the observation that at this time of the day, the lightning frequency derived from 7 y of measurements performed by the LIS- and the OTD-instrument reaches its maximum.[27] In summary each of the trajectories being considered by BRAPHO is initialised according to the conditions at its starting point with respect to emissions from vegetation and fire activity. For lightning trajectories, the local time is considered.

In order to compare the model results with trace gas columns derived from GOME measurements, the modeled volume mixing ratios of O$_3$, NO$_2$ and HCHO are converted into trace gas columns. This is done by projecting the concentration of each species into a three dimensional grid, which accounts for the trajectory's current horizontal position and its altitude. Since the majority of species experience a diurnal photochemical cycle, their volume mixing ratios are extracted at 1030 local time, which corresponds to GOME's equator-crossing time.

Total tropospheric columns of O$_3$, NO$_2$ and HCHO resulting from biomass burning, biogenic emissions and lightning are derived by performing one model run for each of the individual emission processes. For each of these model runs, the trace gas concentrations of all species considered, $c(p)$, are evaluated as a function of geolocation and pressure. To obtain total tropospheric trace gas columns, the excess columns resulting from all emission processes are superimposed and the tropospheric background column of each species is added.

The excess columns are derived by the integration of the excess concentrations $c_{\mathrm{excess}}(p)$ with respect to pressure p. The excess concentrations are given by the difference between the species' current concentration $c(p)$ and its background concentration $c_{\mathrm{background}}(p)$. The species' background concentrations are derived by a background model run where the model is initialised with unpolluted air masses. These background runs are performed at ten different altitudes throughout the whole troposphere and the lower stratosphere. At each altitude the model is run for several days to allow the chemistry to stabilise.

To account for the joint impact of several emission processes, the modeled excess columns derived for the individual emission processes are superimposed for each considered trace gas. To yield total tropospheric columns, a reference sector value is added. The O$_3$ background column is derived from the background chemistry run and is approximately 21 DU. The tropospheric NO$_2$ background column is about 2.5×10^{14} molecule cm^{-2}.

In Fig. 9 the modeled total tropospheric columns of O_3, NO_2 and HCHO resulting from biomass burning, biogenic emission and lightning are shown.

The modeled ozone columns are generally about 10 DU higher than those retrieved from GOME. In addition the low ozone columns in the centre of the southern part of Central Africa are not well reproduced by the model. This may be due to high aerosol (smoke) loading in the vicinity of the vegetation fires, which may lead to a reduction of the retrieved ozone columns. The southern edge of enhanced ozone columns seems to be shifted too far to the south, as expected from the trajectory analysis and the enhanced ozone columns over the Indian Ocean in the latitudinal region between 10 and 20° S are not well reproduced by the chemical model. The Indian Ocean plumes are explained by a trajectory analysis performed in ref. 35 and a 3D model study,[27] which both show that the plume of O_3 over the Indian Ocean in September 1997 is caused by mixing of air masses from Africa and Indonesia.

Over the African continent the modeled tropospheric NO_2 columns capture the general structure of the spatial distribution of the retrieved tropospheric NO_2 columns. The magnitude of the modeled NO_2 columns is comparable to the retrieved columns. However as noted in the discussion of the trajectory analyses, the main route for transport of significant amounts of NO_2 and the other species is shifted further south in the model. It also appears that the modeled NO_2 columns decay faster than the retrieved columns. The main loss process for NO_x is the pressure dependent reaction of OH with NO_2. This behaviour is therefore either explained by a too rapid loss (*e.g.* an inaccurate OH field) or by the presence of sources of NO_x, which are either inadequately modeled or not considered on the model. In this context the modeling of production and deposition of HNO_3 is critical. NO_x is lost by the reaction of N_2O_5 at night on aerosols. HNO_3 is soluble and both its dry and wet deposition needs further investigation. The maximum NO_2 is somewhat higher in the model than that retrieved from GOME. This may be the result of an effective smearing in the east–west direction of the GOME value. This results from the dimension of the 40×320 km^2 ground scene. The modeled plume of NO_2 flowing off the Atlantic coast from the Congo basin does not extend as far and is not so pronounced as that retrieved from GOME. This is probably indicating limitations in the modeling of the NO_2 sources and sinks as well as limitations the meteorological data set. The lightning over the ocean is one likely source. In the savannah regions of North and West Africa, the modeled NO_2 are somewhat lower than that from GOME. This may be a result of pollution and soil emissions, which are not the focus of this study.

The modeled HCHO columns pick out the prominent features of the distribution of the column amount retrieved from GOME measurements. However over the African continent, retrieved enhanced HCHO columns are located north of about 15° S whereas modeled HCHO columns are enhanced north of about 25° S.

The difference between modeled and retrieved total HCHO columns is shown in Fig. 10. Over the dense tropical rain forest modeled and retrieved HCHO columns agree reasonably well in magnitude. In these regions the model tends to underestimate the retrieved HCHO columns in the order of up to 2×10^{15} molecule cm^{-2}, which is in the order of the fitting uncertainty. Over the tropical Atlantic the differences between measured and retrieved HCHO columns also remain in the order the fitting error. Another important factor, which might explain in part differences in HCHO, is the modeling of the isoprene emission. In reality these emissions are not homogeneously distributed over an entire vegetation regime as assumed in our model. The flux of isoprene is strongly related to the leaf area, the temperature and the humidity.

Over the desert areas at the western coast of Africa, the model overestimates the retrieved HCHO columns. As a result of the low level of cloudiness in this region, the quality of any trace gas retrieval is expected to be good for this region. Consequently the large deviations between modeled and retrieved trace gas columns are likely to be related to an inaccurate transport, determined from the meteorological data in south-west Africa.

6. O_3, NO_2 and HCHO columns and the impact of biomass burning and biogenic emissions on HCHO

In order to estimate the relative importance of the different emission trajectory types for the O_3, NO_2 and HCHO amounts produced along the trajectories, the total amount of substance was integrated and the mass determined. For O_3 and NO_2 the amount in the region, defined by the
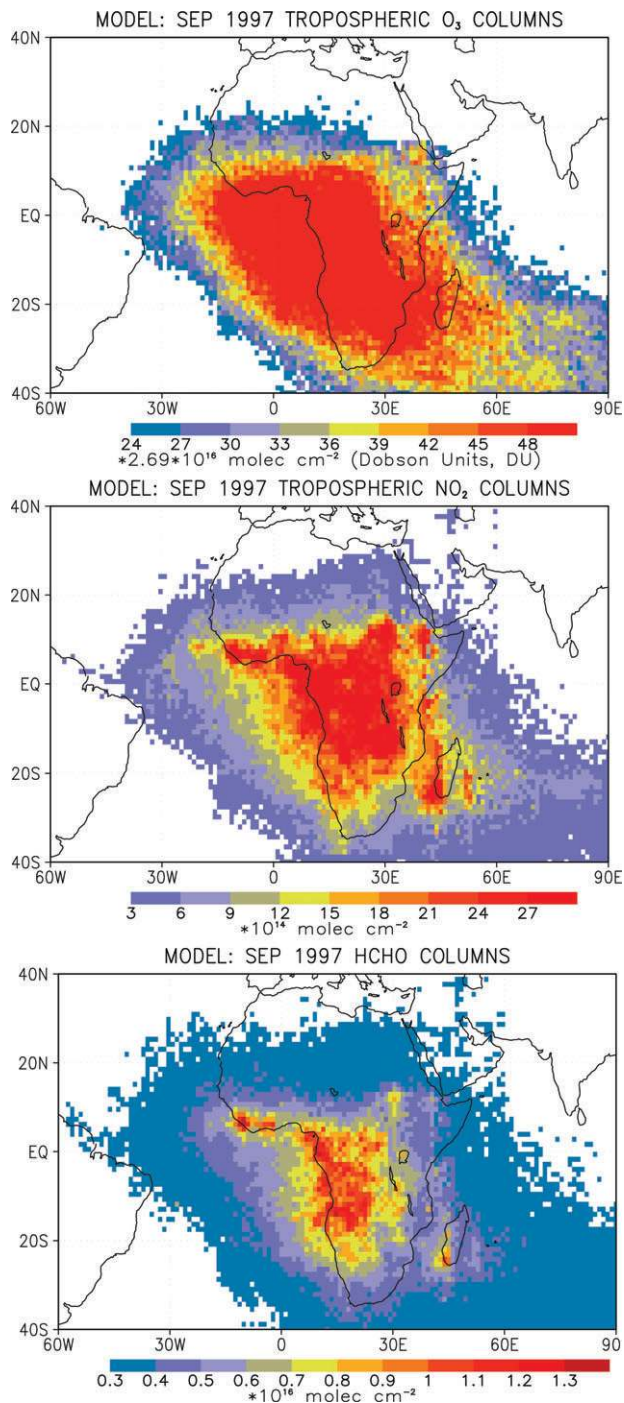
Fig. 9 O$_3$, in DU, NO$_2$ (in 10^{15} molecule cm^{-2}) and HCHO (in 10^{16} molecule cm^{-2}) in for September 1997.

longitudes from 30° W to 90° E and the latitudes 25° S to 10° N, was calculated. This approach avoided the anthropogenic pollution from South Africa and the South American biomass burning
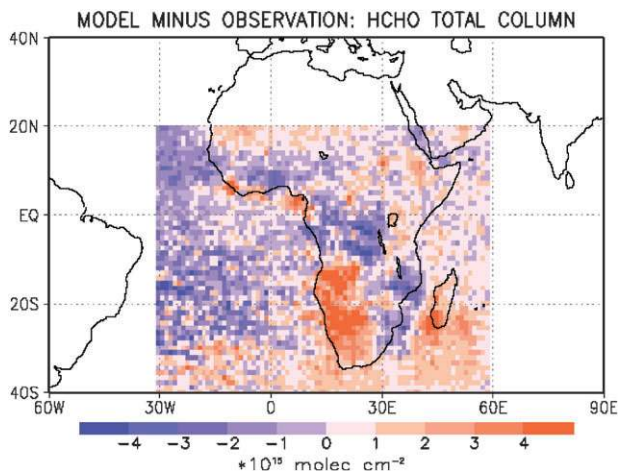
MODEL MINUS OBSERVATION: HCHO TOTAL COLUMN

Fig. 10 The difference $(TC(HCHO)_{model} - TC(HCHO)_{GOME}$ in units of 1×10^{15} molecule cm^{-2}) between modeled total HCHO columns and HCHO columns, retrieved from GOME measurements.

plumes, which are clearly visible in GOME. For HCHO the integration region was chosen to be $20°$ W to $60°$ E and $40°$ S to $20°$ N.

Table 1 contains the tropospheric excess amounts of O_3, NO_2 and HCHO calculated along biomass burning, biogenic emission (two types) and lightning trajectories and the total.

The integration along the modeled trajectories results in about two thirds of the O_3 over Africa being generated by biomass burning in the model. The lightning trajectories play a minor role: less than 10% of the modeled excess O_3 being produced along these trajectories. In comparison roughly half of the NO_2 is produced by biomass burning and one-third results along lightning trajectories.

Compared to GOME observation,

(i) the model underestimates the amount of excess O_3 over Africa,

(ii) the model overestimates the amount of excess NO_2,

(iii) the amount of HCHO appears to be in reasonable agreement.

The inaccuracies in transport may be playing a role, but for this analysis it is assumed that errors in transport are not a significant source of error for the calculation of the total excess amount of the substance. Similarly we shall assume that the tropospheric excess from GOME within its error has no systematic bias. On this basis, the difference between model and GOME excess NO_2 amount, *i.e.*

Table 1 Modeled and observed excess amounts of O_3, NO_2 und HCHO due to biomass burning, biogenic emissions and lightning in comparison to GOME observation. All trace gas amounts are given in Tg

| Source	Trace gas amount/Tg		
	O_3	NO_2	HCHO
Biomass burning	20.4	0.027	0.028
Biogenic emission (tropical rainforest)	8.5	0.011	0.020
Biogenic emission (woody savannah)	1.9	0.0025	0.013
Lightning	2.3	0.013	0.0040
Modeled excess trace gas amount (considering all sources)	33.0	0.054	0.065
Stratospheric–tropospheric exchange	0.42	n/a	n/a
Observed excess trace gas amount (GOME)	51.0	0.0258	0.075
Model : observation ratio	0.65	2.1	0.87
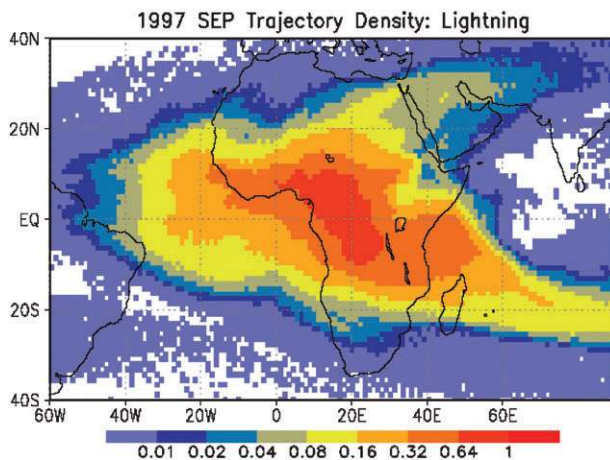
Fig. 11 Trajectory density for trajectories emerging from lightning during September 1997.

the overestimation, is potentially significant. It may be explained by either the NO_2 source being too large or the chemical loss of NO_x being underestimated in the model. If an inaccurate loss of NO_x is the main cause for this difference then a larger boundary layer/lower tropospheric loss of NO_2 is more plausible than one in the upper troposphere. In addition the pattern of the NO_2 seems to indicate that the lightning NO_x emission in the model is overestimating the NO_2. The trajectory density for lightning trajectories is shown in Fig. 11.

The underestimation of the tropospheric O_3 in the model may in a significant part be a result of the omission of trajectories coming from the stratosphere. Trajectory calculations indicate significant entrainment of stratospheric air masses into the troposphere over the southern parts of Africa but this needs further investigation. The apparent good agreement for the HCHO is either fortuitous or reflects the fact that the decay of VOC is reasonably well modeled. The overestimation of NO_2 and the underestimation of O_3 by the model may also be linked with the respect to the efficiency and effective chain length of the production for O_3 production in the model. In addition Table 1 shows an estimate of the amount of the tropospheric excess of O_3 calculated for strato-spheric–tropospheric exchange (STE). The influence of trajectories which pass through the stratosphere was used to make this estimate.

The tropospheric column of HCHO is expected to be mainly located in the lower troposphere because of several effects *e.g.*:

(a) the emission of HCHO precursors (NMHC/VOC) (*e.g.* from biomass burning, by plants or by anthropogenic activity) mainly takes place at the earth's surface,

(b) the oxidation of many of these NMHC/VOC is rapid,

(c) the lifetime of HCHO primarily arising from reaction with OH and photolysis is also relatively short.

(d) the photolysis frequency of HCHO increases as a function of height. (Based on own box model studies, the HCHO lifetime close to the ground is in the order of about 4 h, whereas at 5 km altitude its lifetime is already halved.)

Both biomass burning and biogenic emission lead to enhanced HCHO columns. The relevance of both processes with respect to HCHO has been investigated by determining from the model the vertical excess HCHO columns induced by each of the emission processes.

The excess HCHO columns being produced as a result of biomass burning in the model are shown in Fig. 12 (top), those induced by biogenic emissions in Fig. 12 (bottom). The excess columns of both processes are comparable in magnitude taking the uncertainties in the emissions into account: the total amount of HCHO generated by biogenic emission (0.033 Tg) exceeding the amount generated by biomass burning (0.028 Tg) by a factor of about 1.2.

During September 1997 biomass burning activity was mainly located in the south of central Africa (ZZM-region) (see Fig. 2). HCHO induced by biomass burning is spread over the entire
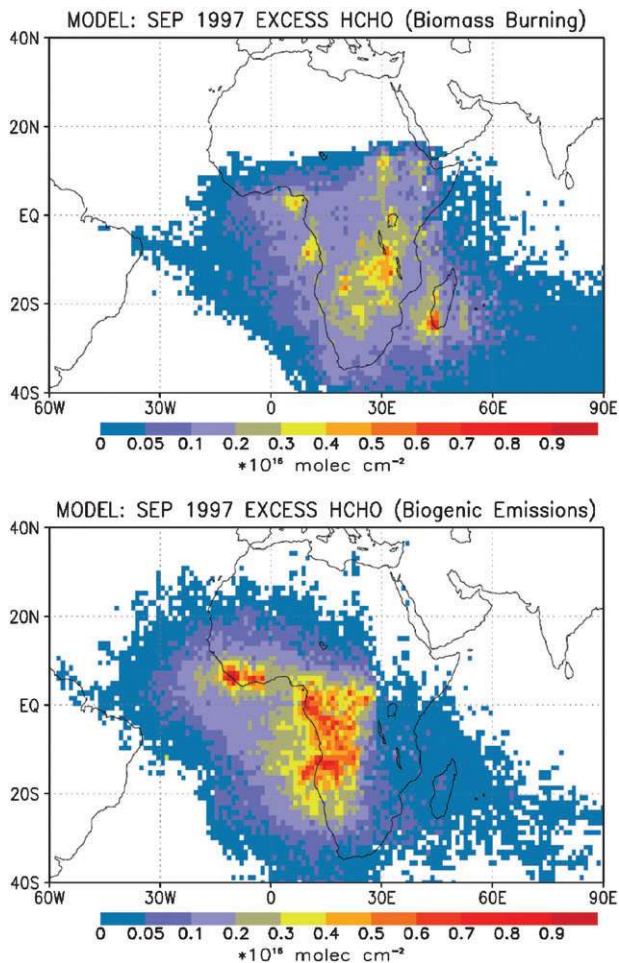
Fig. 12 Excess HCHO columns: resulting from (a) biomass burning, shown above, and (b) biogenic emission, shown below, in units of 10^{16} molecule cm^{-2} for September 1997.

south of Africa whereas HCHO generated by biogenic emissions of the tropical rain forest is strongly localised to its source region.

These differences in the spatial distribution of HCHO columns from the two sources are attributed primarily to the differences in the transport of air masses between the tropics and the subtropics, as discussed above. Additionally the chemistry of VOC being emitted from forests (which is mainly isoprene) differs from the chemistry of VOC being released by biomass burning, which in comparison comprise much more slowly reacting NMHC (mainly $<C_3$). The lifetime of isoprene for its reaction with OH has been estimated to be of the order of 35 min. In comparison the lifetime of many of the VOC emitted by biomass burning is in the order of several hours to days.[11] Thus the VOC emitted by biomass burning is oxidised to HCHO over much larger distances than the biogenic VOC. This behaviour coupled with the differences in convection and advection results in the HCHO from the oxidation of VOC from biomass burning in Africa in September 1997 being transported over a larger area than the HCHO from the biogenic emissions. Further the isoprene emission from the tropical rain forest results in enhanced HCHO columns throughout the year (see Fig. 4) whereas the biomass burning is subject to a significant annual cycle with respect to activity and spatial distribution.

7. Conclusions

During September 1997 tropospheric columns of O_3, NO_2 and HCHO retrieved from GOME measurements show large and enhanced columns over the African continent, the tropical Atlantic Ocean and parts of the Indian Ocean. Maximum tropospheric columns of about 45 DU of O_3, 2.7×10^{15} molecule cm^{-2} of NO_2 and of up to 1.2×10^{16} molecule cm^{-2} of HCHO are retrieved over the atmospheric scene observed by GOME. This behaviour is explained by the transport and transformation of emissions of VOC and NO_x from biomass burning, lightning and biogenic emissions. This has been investigated by a trajectory analysis and a study using a Lagrangian chemical model to simulate the chemistry along the trajectories.

From the trajectory analysis, the spatial distribution of the enhanced trace gas columns are qualitatively reasonably well reproduced. However the emissions from biomass burning are generally shifted to the south with respect to the pattern retrieved from GOME. This is considered to be most likely the result of inaccuracies within the ERA-40 meteorological data in the middle and upper troposphere. This may be a result of the lack of observations in the tropics, which are used as input for the ERA-40.

To study the chemical transformation along the trajectories, the chemical box model BRAPHO has been applied to simulate the chemical behaviour along a large number of trajectories emerging from the regions having biomass burning or biogenic emissions. Fluxes to or from soils have not been considered explicitly in this study. The main advantage of this joint transport and chemistry analysis is that the impact of an individual emission process and its transport can be investigated qualitatively by the trajectory analysis and quantitatively by the chemistry model. All emission processes can be treated independently from each other. The resulting modeled tropospheric trace gas columns of O_3, NO_2 and HCHO are comparable with the columns retrieved from GOME measurements with respect to trace gas amounts and their spatial distribution. The enhanced trace gas columns of O_3, NO_2 and HCHO seem to be shifted too far south, which we attribute to the inaccuracies in the ERA-40 data set consistent with the trajectory analysis.

For September 1997 the model calculations indicate that similar amounts of HCHO are generated from biomass burning (0.028 Tg) and biogenic emissions (0.033 Tg). The reactions of the biogenic NMHC/VOC are rapid compared to those from the biomass burning and the transport out of the regions of biogenic emission is effectively slower than that from biomass burning regions. As a consequence the HCHO columns are relatively large and located close to and slightly downwind of the biogenic source regions such as the dense tropical rain forests. In contrast the biomass burning emissions are convected and as a result advected over a significantly wider region.

References

1 J. P. Burrows, M. Weber, M. Buchwitz, V. V. Rozanov, A. Ladstätter-Weißenmayer, A. Richter, R. de Beek, R. Hoogen, K. Bramstedt, K.-U. Eichmann, M. Eisinger and D. Perner, *J. Atmos. Sci*, 1997, **56**, 151.
2 A. M. Thompson and R. D. Hudson, *J. Geophys. Res.*, 1999, **104**, 26961.
3 D. P. Edwards, J.-F. Lamarque, J.-L. Attie, L. K. Emmons, A. Richter, J.-P. Cammas, J. C. Gille, G. L. Francis, M. N. Deeter, J. Warner, D. C. Ziskin, L. V. Lyjak, J. R. Drummond and J. P. Burrows, *J. Geophys. Res.*, 2003, **108**, DOI: 10.1029/2002JD002927.
4 C. Granier and G. Brasseur, *Geophys. Res. Lett.*, 2003, **20**, 1086.
5 J. van Aardenne, F. J. Dentener, J. G. J. Olivier, C. G. M. Klein Goldewijk and J. Lelieveld, *Global Biogeochem. Cycles*, 2001, **15**, 909.
6 P. J. Crutzen, L. E. Heidt, J. P. Krasnec, W. H. Pollock and W. Seiler, *Nature*, 1979, **282**, 253.
7 P. J. Crutzen and M. O. Andreae, *Science*, 1990, **250**, 1669.

8   S. J. Oltmans, A. S. Lefohn, H. E. Scheel, J. M. Harris, H. Levy II, I. E. Galbally, E.-G. Brunke, C. Meyer, J. A. Lathrop, B. J. Johnson, D. S. Shadwick, E. Cuevas, F. J. Schmidlin, D. W. Tarasick, H. Claude, J. Kerr, O. Uchino and V. Mohnen, *Geophys. Res. Lett.*, 1998, **25**, 139.
9   J. Fishman and P. J. Crutzen, *Nature*, 1978, **274**, 855.
10 R. Atkinson, *Atmos. Environ.*, 2000, **34**, 2063.
11 J. H. Seinfeld and S. N. Pandis, *Atmospheric Chemistry and Physics*, Wiley-VCH, Weinheim, 1st edn., 1997.
12 T. Fehr, *Mesoskalige Modellierung der Produktion und des dreidimensionalen Transports Stickoxiden durch Gewitter*, PhD Thesis, Ludwig Maximilian University, Munich, 2000.
13 A. Richter, *Absorptionsspektroskopische Messungen stratosphärischer Spurengase über Bremen, 53 N*, PhD thesis, University of Bremen, 1997.
14 A. Richter and J. P. Burrows, *Adv. Space Res.*, 2002, **29**, 1673.
15 A. Ladstätter-Weißenmayer, J. P. Burrows and D. Perner, *Earth Obs. Q.*, 1999, **58**, 28.
16 W. Thomas, E. Hegels, S. Slijkhuis and R. Spurr, *Earth Obs. Q.*, 1998, **58**, 30.
17 K. Chance, P. Palmer, R. J. D. Spurr, R. V. Martin, T. P. Kurosu and D. J. Jacob, *Geophys. Res. Lett.*, 2000, **27**, 3461.
18 J. C. Fishman, E. Watson, J. C. Larsen and J. A. Logan, *J. Geophys. Res.*, 1990, **95**, 3599.
19 J. P. Burrows, 1999, in *Developments in Atmospheric Sciences 24: Approaches to Scaling Trace Gas Fluxes in Ecosystems*, ed. A. F. Bouwman, Elsevier, Amsterdam, pp. 315–347.
20 C. Leue, M. Wenig, T. Wagner, U. Platt and B. Jähne, *J. Geophys. Res.*, 2001, **106**, 5493.
21 A. Ladstätter-Weißenmayer, J. Meyer-Arnek, A. Schlemm and J. P. Burrows, *Atmos. Chem. Phys.*, 2004, **4**, 1773.
22 C. K. Folland and D. E. Parker, *Q. J. R. Meteorol. Soc.*, 1995, **121**, 319.
23 O. Arino, J.-M. Melinotte, J.-M. Rosaz and E. Monjoux, ESA Fire Product, *Proceedings of the 7th ISPRS conference on Physical Measurement and Signatures in Remote Sensing*, Courchevel, 1997.
24 O. Arino, J.-M. Rosaz and J.-M. Melinotte, *Proceedings of the IUFRO Conference on Remote Sensing and Forest Monitoring*, Rogow, Poland, 1999, June 1–3.
25 T. R. Loveland, B. C. Reed, J. F. Brown, D. O. Ohlen, Z. Zhu, L. Yang and J. W. Merchant, *Int. J. Remote Sens.*, 2000, **21**, 1303.
26 H. J. Christian, R. J. Blakeslee, D. J. Boccippio, W. L. Boeck, D. E. Buechler, K. T. Driscoll, S. J. Goodman, J. M. Hall, D. M. Mach and M. F. Stewart, *J. Geophys. Res.*, 2003, **108**, DOI: 10.1029/2002JD002347.
27 T. Kunhikrishnan, M. G. Lawrence, R. von Kuhlmann, A. Richter, A. Ladstaetter-Weissenmayer and J. P. Burrows, *Geophys. Res. Lett.*, 2004, **31**, L08110, DOI: 10.1029/2003GL019269.
28 G. D. Carver, P. D. Brown and O. Wild, *Comput. Phys. Commun.*, 1997, **105**, 197.
29 J. C. Fishman, J. M. Hoell, R. D. Bendure, R. J. McNeal and V. W. J. H. Kirchhoff, *J. Geophys. Res.*, 1996, **101**, 23865.
30 S. M. Saunders, M. E. Jenkin and R. G. Derwent, *Atmos. Chem. Phys.*, 2003, **3**, 161.
31 A. B. Guenther, R. K. Monson and R. Fall, *J. Geophys. Res.*, 1991, **96**, 10799.
32 M. G. Sanderson, *Monoterpenes, Ethene and Propene by Vegetation, Technical note 40*, Hadley Centre, Reading, 2002.
33 J. P. Greenberg, A. B. Guenther, S. Madronich, W. Baugh, P. Ginoux, A. Druilhet, R. Delmas and C. Delon, *J. Geophys. Res.*, 1999, **104**, 30659.
34 S. Sillman, M. A. Carroll, T. Thornberry, B. K. Lamb and H. Westberg, *J. Geophys. Res.*, 2002, **107**, DOI: 10.1029/2001JD000449.
35 A. Ladstätter-Weißenmayer, J. Meyer-Arnek, A. Richter, F. Wittrock and J. P. Burrows, *Atmos. Chem. Phys.*, 2005, submitted.